ORIGINAL PAPER - EXPLORATION GEOLOGY

CrossMark

Reservoir characteristics and three-dimensional architectural structure of a complex fault-block reservoir, beach area, China

Xue Li[1] · Ning Zhou[1] · Xing Xie[1]

Abstract

The objective area in this paper is a complex fault-block reservoir, which is provided by China Petroleum Engineering Design Competition. Reservoir characteristics which comprise of stratigraphic features, vertical changes, and section properties (thickness, percentage sand, and percentage amalgamation) are documented. Through comprehensive analysis on structural architecture and reservoir characteristics, a three-dimensional quantitative reservoir modeling is taken at a regional scale of $69 \times 97 \times 37 \ m^3$ with the application of geostatistics as theoretical guidance. Then, a high-resolution hierarchical reservoir model of this field has been generated with a combination of hierarchical, structural, physical, and well trajectory data. The established three-dimensional geological model integrates all well and structural information, which can provide a basic model for subsequent sedimentary microfacies modeling and property modeling as well. Finally, a series of profiles are built successively, they are three-dimensional fence diagrams, connecting well sections and well group profiles, which can be a valuable tool for reflecting geologic body with great reality and thus achieve reservoir characterization of the complex fault-block reservoir.

Keywords Reservoir characteristics · Architectural structure · Fault-block reservoir · Three-dimensional modeling

Introduction

To represent spatial objects in three-dimensional space, the related three-dimensional model or data structures have been investigated, such as grid system, linear octree, fence diagram, and tetrahedron network (TEN) (Pilout et al. 1994; Chen et al. 1995; Houlding 1994; Martinez et al. 2017). There are many varieties of geological models generated from different modeling methods and geologists (Soubeyrand 2017; Mery et al. 2017). Geological modeling often refers to raster-based or vector-based models, both of which have its own features and applicability. The description of 3D objects is aimed at skeleton modeling, surface modeling, inner modeling, and property modeling, and thus geological data need to be considered as much as possible (González-Garcia and Jessell 2016), including cores, outcrops, logs, seismic data, test data, boreholes, maps, and so on (Bourdeau et al. 2017). Meanwhile, fence diagram and profiles

which can represent the inner structure of a geological body are the two issues of crucial importance (Lemon and Jones 2003; Turner and Gable 2003), as this allows a geologist to understand the geological interior structure and optimize development schema accordingly. Therefore, it is worth conducting detailed studies on reservoir characteristics and three-dimensional architectural structure of the study area.

In this paper, based on geometric volume modeling, minimum curvature interpolation, and arithmetic and harmonic methods, a regional three-dimensional geological model is established in accordance with the complexity of geological entities. Profiles and fence models are accordingly built in order to display the characteristics of internal geologic body in detail.

Geological setting

The study area covers an area of 5.5 km², which is about 1858 m wide from east to west and 2980 m long from north to south. The distance between the study area and the nearest oil storage is 120 mile, and the regional water depth ranges

---

✉ Xue Li
   lix@cczu.edu.cn

[1] School of Petroleum Engineering, Changzhou University, Changzhou 213164, China

مدينة الملك عبدالعزيز
KACST للعلوم والتقنية

 Springer

from 1350 to 1525 m. The regional terrain map is shown in Fig. 1a.

Tectonic characteristics

The study area is a NE-trending semi-anticlinal reservoir, which is complicated by faults within the study area (Fig. 1b). The eastern boundary fault runs through the whole study area and produces a series of EW-trending faults, followed by well-developed fault zone consequently.

The fault activity is relatively stronger during sedimentary period of CPEDC3 and CPEDC2, and weakens in other sedimentary period. There area total of three groups of faults: One group is the eastern boundary fault which is in NE trending throughout the whole study area and thus controls the regional structure and sedimentary evolution; another group is a NEE trending fault which extends from 4.3 to 6.4 km with the fault displacement of 180–740 m, and the fault displays echelon arrangement; others are secondary faults with characteristics of small fault displacement and short extended distance, which makes the regional structure more complicated.

Regional stratigraphy

The formations of the study area, in decreasing age order, are A formation of Quaternary, B1 and B2 formations of Neogene, and C1 and C2 formations of Paleogene, respectively. The main oil-bearing formation is the third member of C2 formation (CPEDC3). The formation characteristics of the study area are shown in Fig. 2.

The C2 set can be divided into four formations; in decreasing age order, they are the first member of CPEDC formation (CPEDC1), the second member of CPEDC formation (CPEDC2), the third member of CPEDC formation (CPEDC3), and the fourth member of CPEDC formation (CPEDC4), respectively. However, the effective drilling strata include CPEDC1, CPEDC2, and CPEDC3. CPEDC3 can be further subdivided into three sub-members: upper, middle, and lower sub-member.
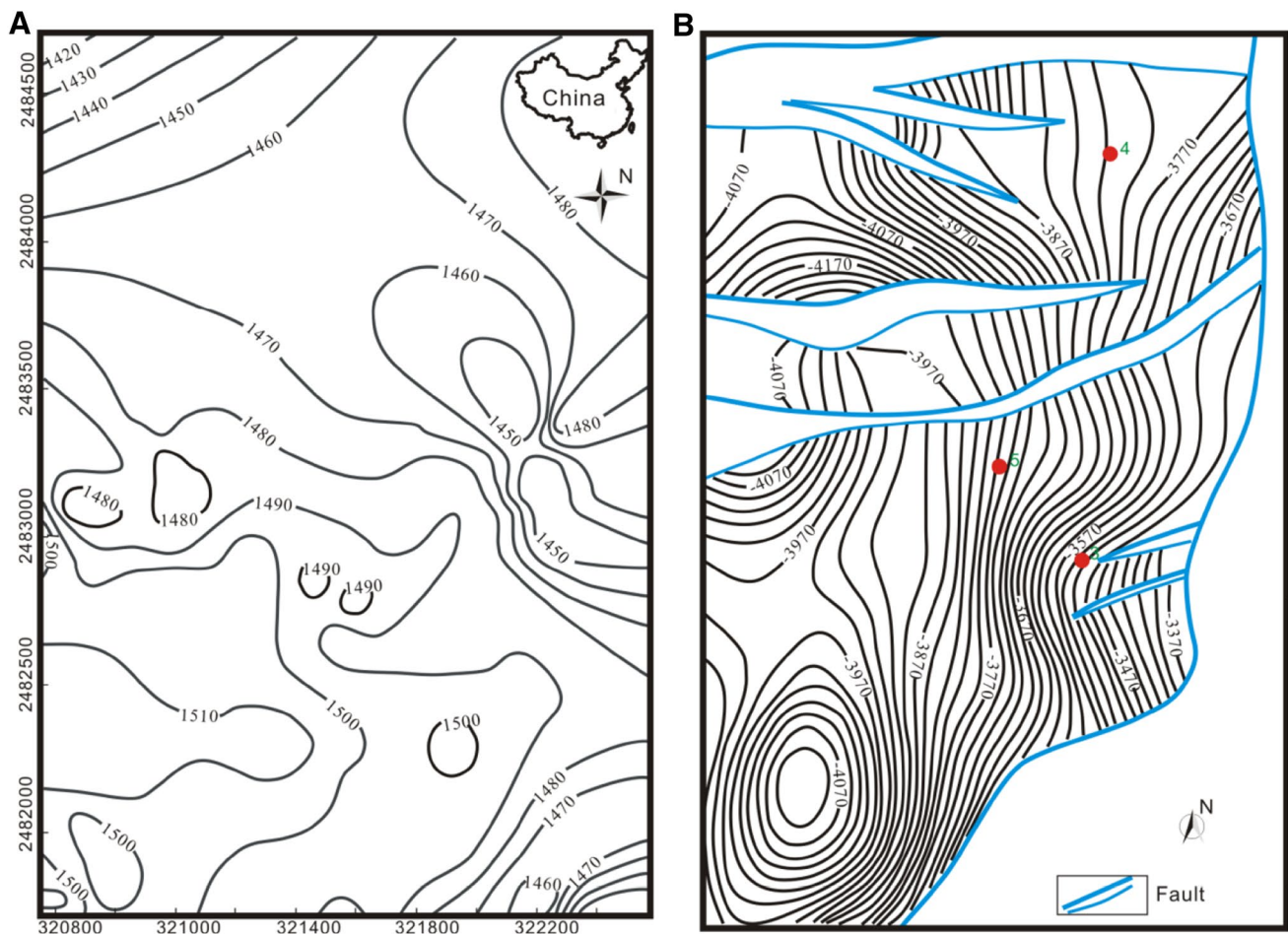
Fig. 1 Geological map of the study area. **a** The terrain map, showing the distribution trend of contour and the surface characteristics as well; **b** the top structure map of the third member of CPEDC, showing the distribution of the faults and the production wells in the study area

Fig. 2 Synthetical stratum histogram of the study area, displaying the main lithologic characteristics and sedimentary sequences from sedimentological interpretation
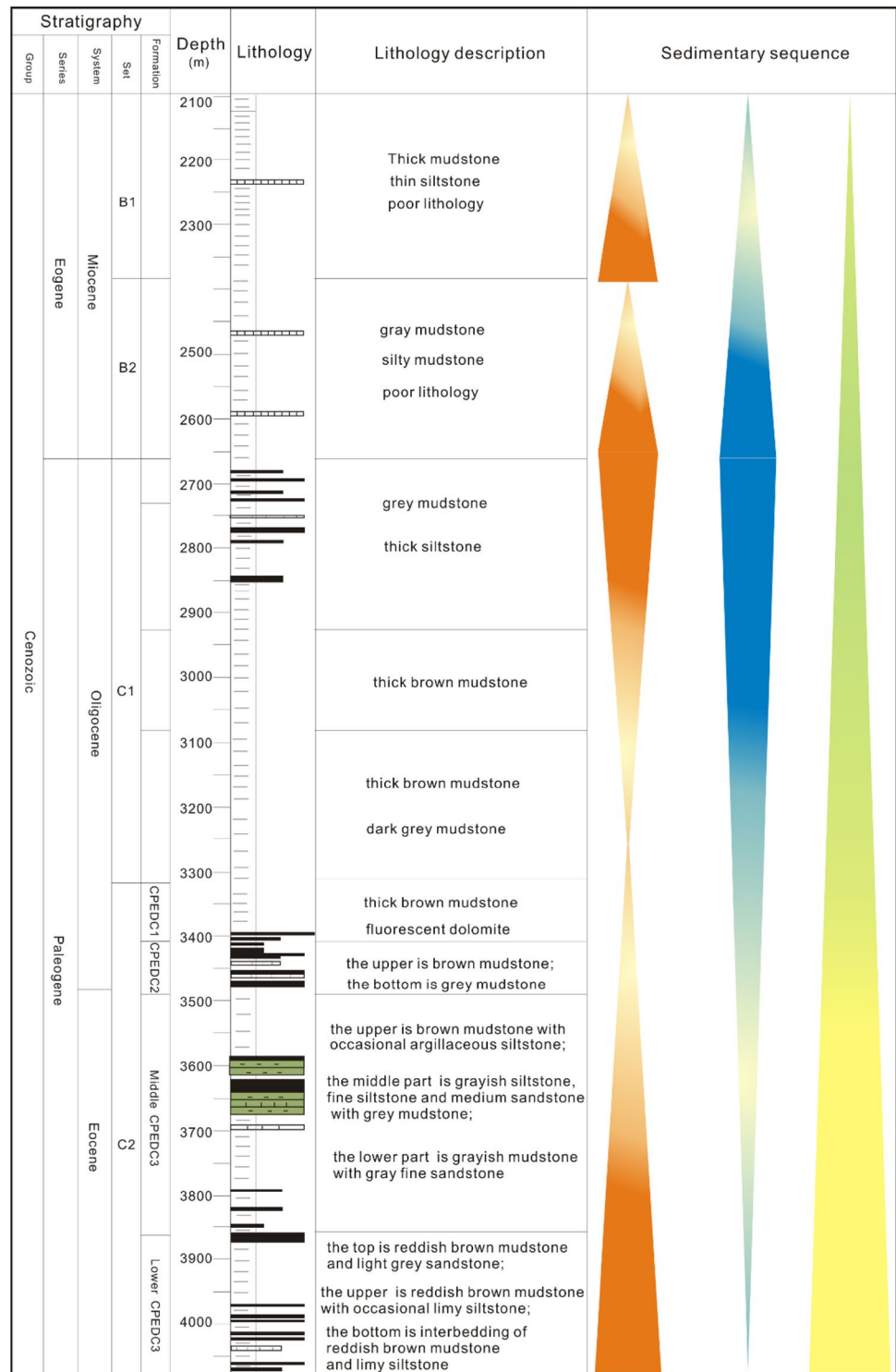
The stratum CPEDC1 ranges in thickness from 60.5 to 157 m, and the dominant lithology of the study area is brownish gray mudstone with little internal calcareous shale. Argillaceous dolomite is developed locally in the study area. In short, CPEDC1 is a set of special lithologic section.

The stratum thickness of CPEDC2 ranges from 41.5 to 115 m. The upper part of CPEDC2 is brownish gray mudstone with a small amount of siltstone. The lower part consists of gray mudstone and lots of light gray fine sandstone and pebbly sandstone interbeddings with different thickness.

The upper part of stratum CPEDC3 is lost. The stratigraphic thicknesses of the middle CPEDC3 displayed by well drilling range between 204.5 and 746.5 m. The main lithology is light gray and brown mudstone, and a set of reservoir develops in the middle layer of mudstone with thickness of 18.5–166.5 m. The lower stratum of CPEDC3 shows many interbeddings of reddish brown mudstone and gray siltstone with different thickness.

Reservoir characteristics

Petrologic characteristics

The main lithology of CPEDC3 is fine-grained sandstone and pebbly coarse sandstone with good sorting and low texture maturity. Petrology is mainly composed of feldspar lithic sandstone and arkoses. The mineral composition includes quartz, feldspar, and debris, with the average content of 33.7, 34.9, and 31.4%, respectively (Fig. 3). The roundness of particles is mainly sub-rounded and sub-angular, and the median particle size is generally between 14 and 479 μm. The X-ray diffraction analysis shows that the primary clay minerals are kaolinite and illite/smectite, which are followed by illite and chlorite.

The lithology of CPEDC2 is dominated by fine-grained sandstone and pebbly coarse sandstone, with medium sorting. Petrology named feldspar lithic sandstone and lithic

feldspathic sandstone, and the main mineral components are quartz, feldspar, and debris, with the average content of 28.5, 39.8, and 31.7%, respectively (Fig. 3). The roundness of particles is mostly sub-rounded and sub-angular, and the median particle size is in the range of 38–461 μm. The X-ray diffraction analysis shows that the most abundant clay minerals are kaolinite and illite/smectite, followed by illite and chlorite.
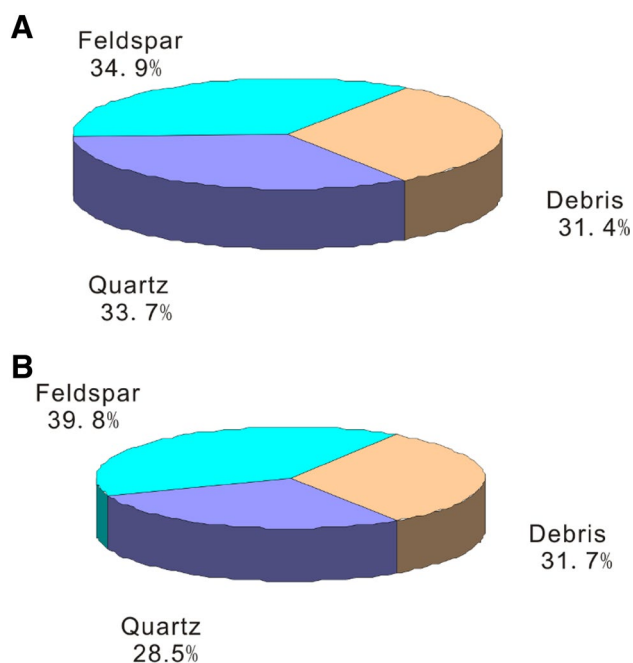
Physical property

The porosity of CPEDC2 is mainly distributed in the 4.5–40.1%, averaging at 22.5%, and the distribution of permeability is between 0.1 and 1687.8 mD, with an average of 267.9 mD.

The capillary curve is mainly coarse slanting degrees with the following characteristics: (1) The drainage pressure is in the scope of 0.013–0.298 MPa; (2) the median saturation pressure is distributed in 0.112–2.433 MPa; and (3) the average pore throat radius ranges from 0.811 to 7.481 μm. The general reservoir characteristic of the study area is medium porosity and medium permeability.

The porosity of CPEDC3 ranges between 9.8 and 34.8%, averaging at 21.3%. And, the permeability is in the distribution of 0.2–3535.1 mD with an average of 382.3 mD.

The capillary curve is basically medium-coarse slanting degrees with the following characteristics: (1) Drainage pressure ranges from 0.013 to 0.997 MPa; (2) median saturation pressure is distributed in the range of 0.098–15.529 MPa; and (3) average pore throat radius is in the scope of 0.198–13.52 μm. The general characteristic of the reservoir in the study area is medium porosity and medium permeability.

Modeling method

The modeling method can be further divided into determinable modeling and stochastic modeling and is used to nicely reflect internal changes of geological body. However, both methods have their own advantages and disadvantages. With the continuous deepening of geological research, an increasing number of uncertain factors in building determinable model are also exposed. In this case, stochastic modeling method can effectively display and evaluate 3D geological model's uncertainty.

1. deterministic modeling

Deterministic modeling, which usually refers to those methods used for construction graph, includes interpolation, Kriging, and geomathematics (Zhang et al. 2007). The reservoir property for the unknown area between wells is assigned

Fig. 3 Reservoir petrologic characteristics of the study area. **a** petrologic characteristics of CPEDC3; **b** petrologic characteristics of CPEDC2

by deterministic modeling, but the premise is to know the basic information of the known wells, then to exactly predict reservoir parameters between wells (Yu 2002). So far, there are mainly three methods which are used for reservoir prediction, they are seismological method, sedimentology method, and Kriging method, respectively. All the three methods belong to deterministic modeling.

The study area is a structural reservoir mainly controlled by the structure and subsidiarily by single sand body. The research is mainly focused on the spatial distribution of structure form through 3D visualization technology.

2. stochastic modeling

In this study, guided by the theory of random function and some known information, a series of optional and equal-possible reservoir models are generated with the use of stochastic simulation method. Indeed, stochastic simulation is a sampling process of extracting the equal-possible part from the stochastic model.

Through comprehensive evaluation on the uncertainty of those stochastic reservoir models, a geological model which coincides with real geological case is consequently defined, then to meet the requirements of oilfield exploration and development decisions within a given risk limit. According to the random characteristics of simulated objects, stochastic model can be divided into three types; they are discrete model, continuous model, and mixed model, respectively. Discrete model is used to describe the geological characteristics with discrete features, such as sand body distribution, microfacies distribution, and fracture or fault distribution. Continuous model is to display the characteristics of continuous changes on reservoir parameters, such as porosity, permeability, and oil saturation.

Actually, the discrete and continuous features both do coexist in reservoir. The mixed model is composed of discrete model and continuous model, which is also named two-step model. The first step is to build discrete model to describe the reservoir heterogeneity characteristics in a wide range, and the second step is to establish continuous model to describe spatial changes and distribution of rock parameters.

Results and discussions

3D integrated structural modeling

The 3D visualization technology and virtual reality technology provide a favorable tool for people to observe and analyze the underground geological body (Shao et al. 2011), which aim to present geological phenomena in 3D space,

such as stratum, structure, and reservoir heterogeneity (Wang et al. 2010).

Modeling data

There are a total of five wells in the study area; they are well1, well2, well3, well4, and well5. The modeling data in this paper involve: (1) well drilling data (including well name, x-coordinate, y-coordinate, and bushing elevation) which is used for describing well location; (2) well trajectory data, which is used for recording well trajectory such as well deviation and azimuth every 30 m; (3) well tops data, which is used for describing drilling horizon and the corresponding depth; (4) well horizon data, which is used for the stratification of the study area; (5) structure map, which is used for digitizing fault and building constraining surface for horizons.
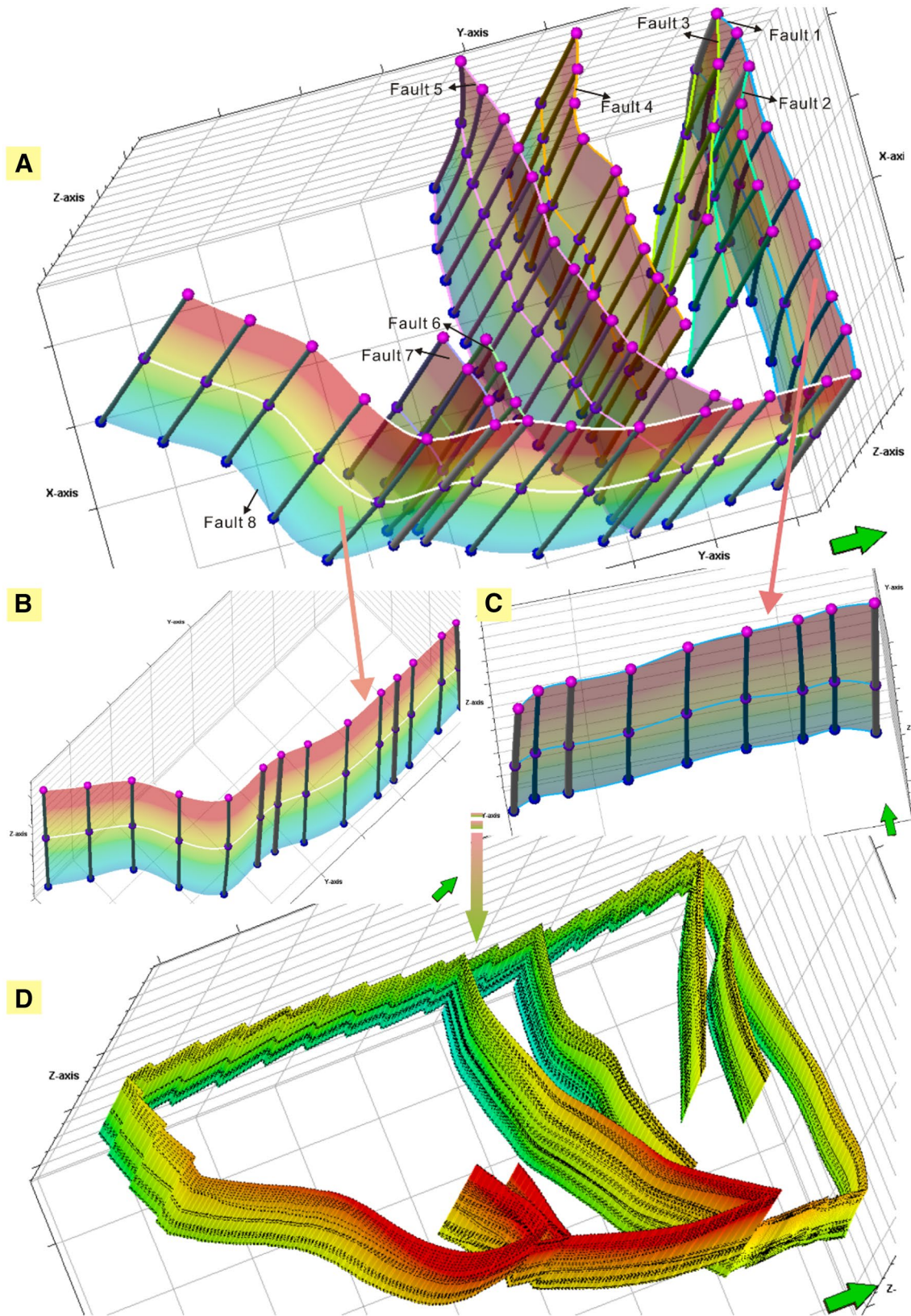
Fault modeling

Three aspects need to be considered in fault modeling: Under what situation can the fault geometry be modeled as a surface (Calcagno et al. 2008); how faults terminate in 3D space and what's the connection relationship between faults; how to properly handle the dip, the angle, the displacement, the relationship between hanging wall and footwall of faults.

1. The two sides of a fault (including hanging wall and footwall) are both digitized from structural map, and then, fault polygons are formed which will be used to define the positions of the fault surface in depth;
2. Fault pillars can be in forms of vertical line, straight line, spade line, or curve comprised of two, three, or five key points, and they are built from fault polygons with fault generated function;
3. Fault dip, azimuth, length, and shape are all defined by fault pillars, and so do other faults of 3D gridding;
4. When all faults are described in detail with the key pillar and have been properly connected, the framework of 3D fault model has been completely established.

There are a total of eight faults in the study area, most of which are intersecting faults. The large fault which is located in the eastern part of the study area is considered as a boundary of fault modeling.

With fault data from fault digitization and human adjustments for faults based on geological analysis, a smooth connection between intersecting faults is accordingly built. 3D model of faults is built by selecting minimum curvature interpolation, which can reflect 3D spatial distribution characteristics and combination features of faults. The 3D fault model of the study area is shown in Fig. 4.

Fig. 4 3D fault model of the study area. **a** regional fault model established with minimum curvature method, showing the spatial distribution and the connection relationship between faults; **b** boundary fault No. 8; **c** boundary fault No. 1; 3D fault surface and the edges of modeling area

Structural model

Structural modeling is a basis and quite important step for the static modeling of reservoir; it can provide three-dimensional skeleton for reservoir property modeling and fluid parameter modeling and thus can be used as a predictive tool for oilfield management and development (Freulon and Dunderdale 1994). In this study, facial modeling method is applied to establish structural model which is composed of geological surfaces and fault surfaces, and consequently generates 3D skeleton of geological body (Shao 2012).

The grid system is 30×30 m in the plane and 0.5 m in the vertical direction with a total number of 3D cells 247,641, which is calculated from $69 \times 97 \times 37$ in I, J, K direction, respectively; the number of 3D nodes is 260,680, which is calculated from $70 \times 98 \times 38$ in *I, J, K* direction, respectively; and the number of 2D cells and 2D nodes is 6693 and 6860, which is calculated from 69×97 and 70×98, respectively. The 2D pillar grid including the middle grid and the base grid is shown in Fig. 5. Through making adjustment on geological surfaces' morphology and their relationships, an integrated 3D structural model is formed by organizing

different blocks which are subdivided by faults (Fig. 6a). In order to display local structure, fence models (Fig. 6b–d), cross-well profile (Fig. 6e), and 3D structural model without taking fault into consideration (Fig. 7) are all built, which are more intuitive in reflecting the internal structure characteristics and connections between different strata.

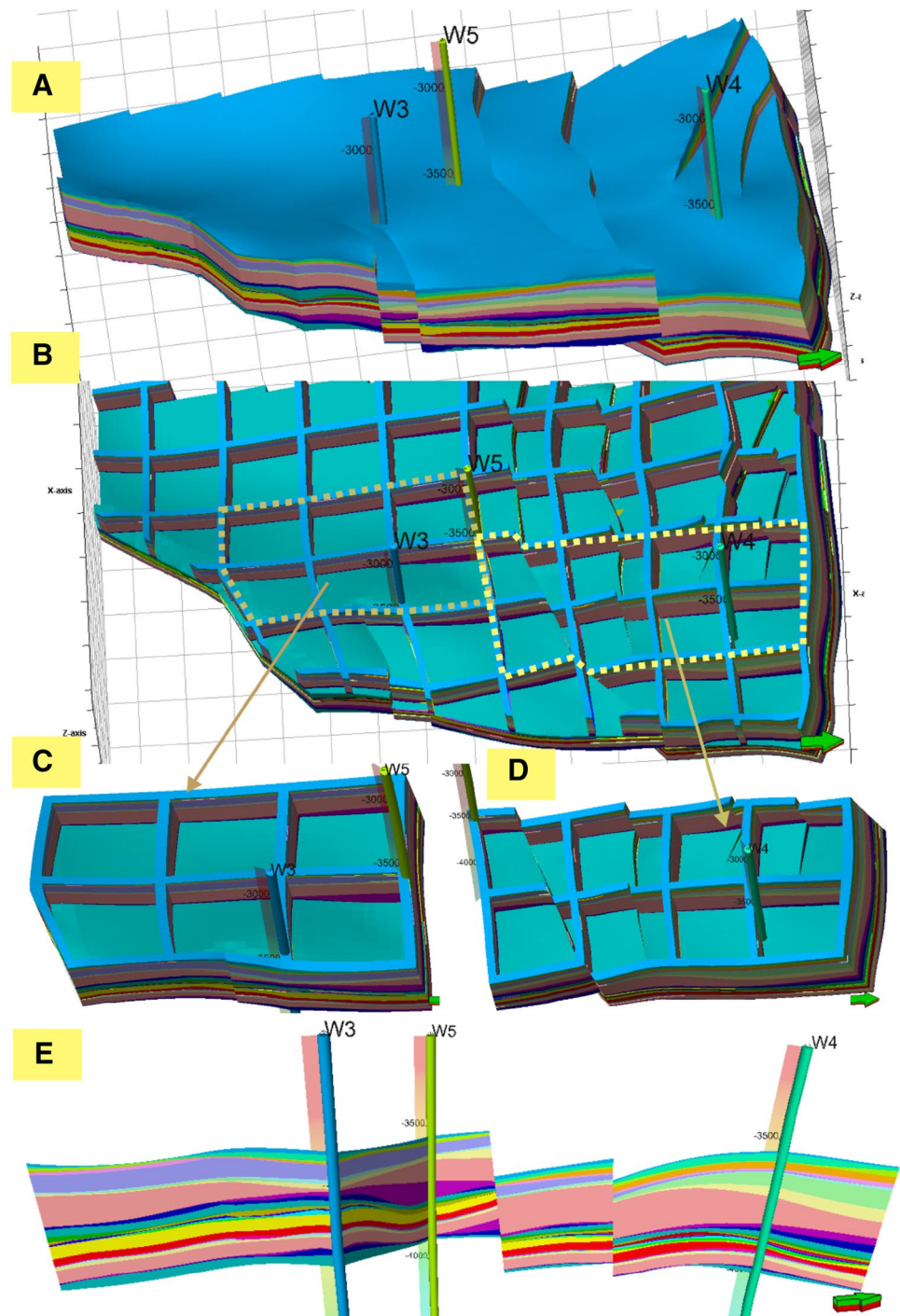## Depositional sand body and property modeling

The CPEDC formation (including CPEDC1, CPEDC2, and CPEDC3) forms the primary target reservoir unit. Deposition of the CPEDC formation was partially controlled by the development of the local rift system with single sedimentary sand body of 8 m thick on average. The porosity has been measured on core material to be between 15 and 30%, the permeability ranges from 10 to 3500 mD, and the shale content is the distribution of 1.5–30%.

A regional sand body model is created from the available sand body data from well point data with sequential indication simulation. Mudstone and the interlayer are both labeled with gray (Fig. 8a, b). At the beginning of property modeling, the most critical step is data analysis
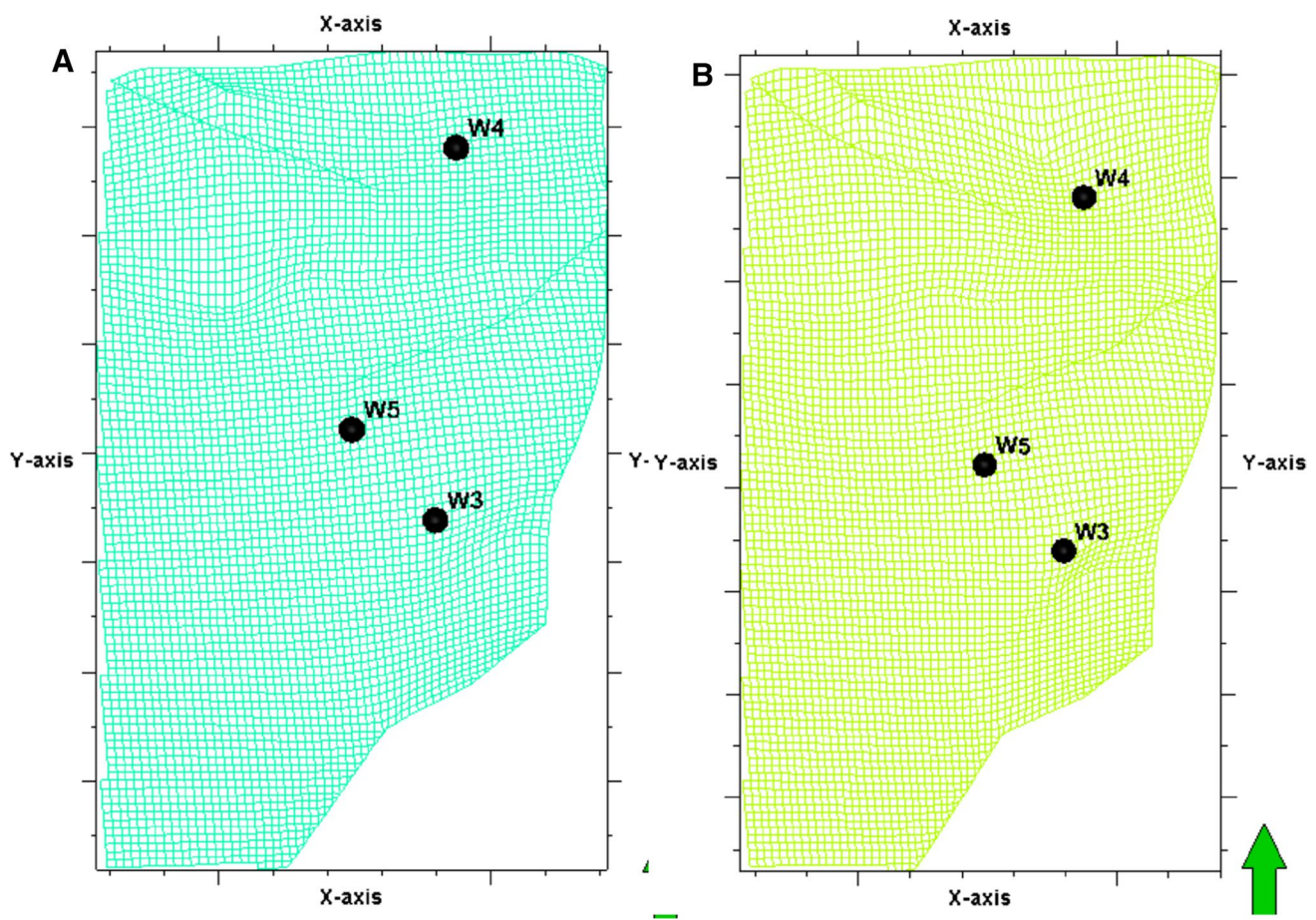
Fig. 5 2D pillar grid of the study area, established with geometric volume modeling method. **a** the middle pillar grid; **b** the base pillar grid

and variation function analysis, in which singular values are truncated to ensure the property data accords with the actual reservoir physical property of the study area. In permeability modeling, singular values which are greater than 3000 are eliminated, and the output data range between 10 and 2000 mD. Based on variation function analysis and adjustment on major range, minor range and vertical range, respectively, the permeability model and the porosity model are established with sequential Gaussian simulation (Chen 2008; Guo and Shi 2008; Hélène and Didier 2016). From 3D porosity model and permeability model and their profiles (Fig. 8c–f), it can be seen that the porosity distribution has good correlation with permeability, which is basically identical to the distribution of sand body, indicating a high reliability of property data analysis and a guarantee for later model simulation accordingly.
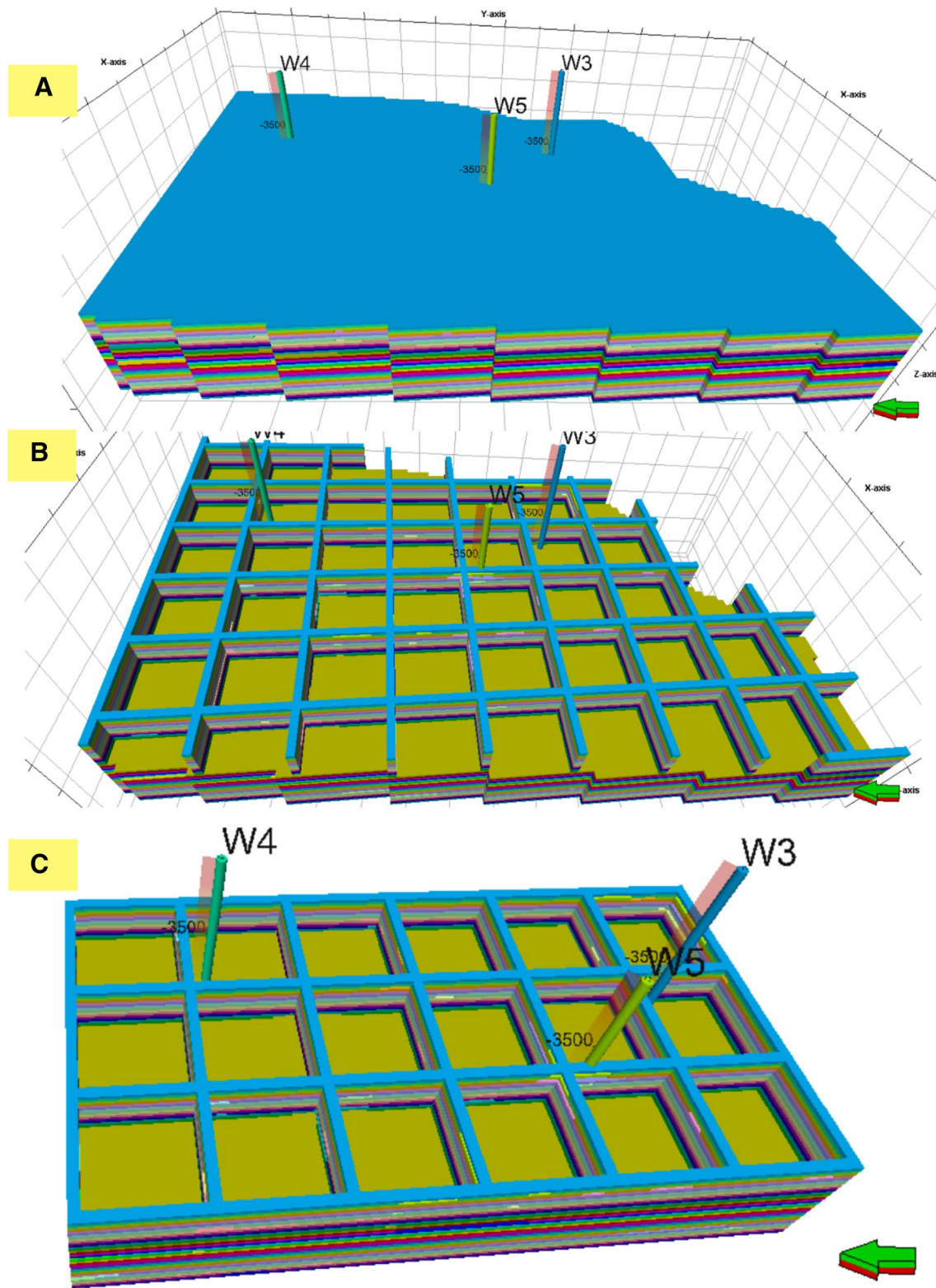
Fig. 7 3D geological model through toggle simbox view, showing the structural model including the fence model without taking fault into consideration. **a** 3D regional geological model of the study area; **b** three-dimensional structural fence model of **a** at X-axis (1, 1, 10), Y-axis (1, 1, 10), and Z-axis (15, 27, 27); **c** zoomed-in views of the left black boxes in **b** at X-axis (56, 1, 1) and Y-axis (23, 67, 1), showing a detailed distribution pattern of structural model
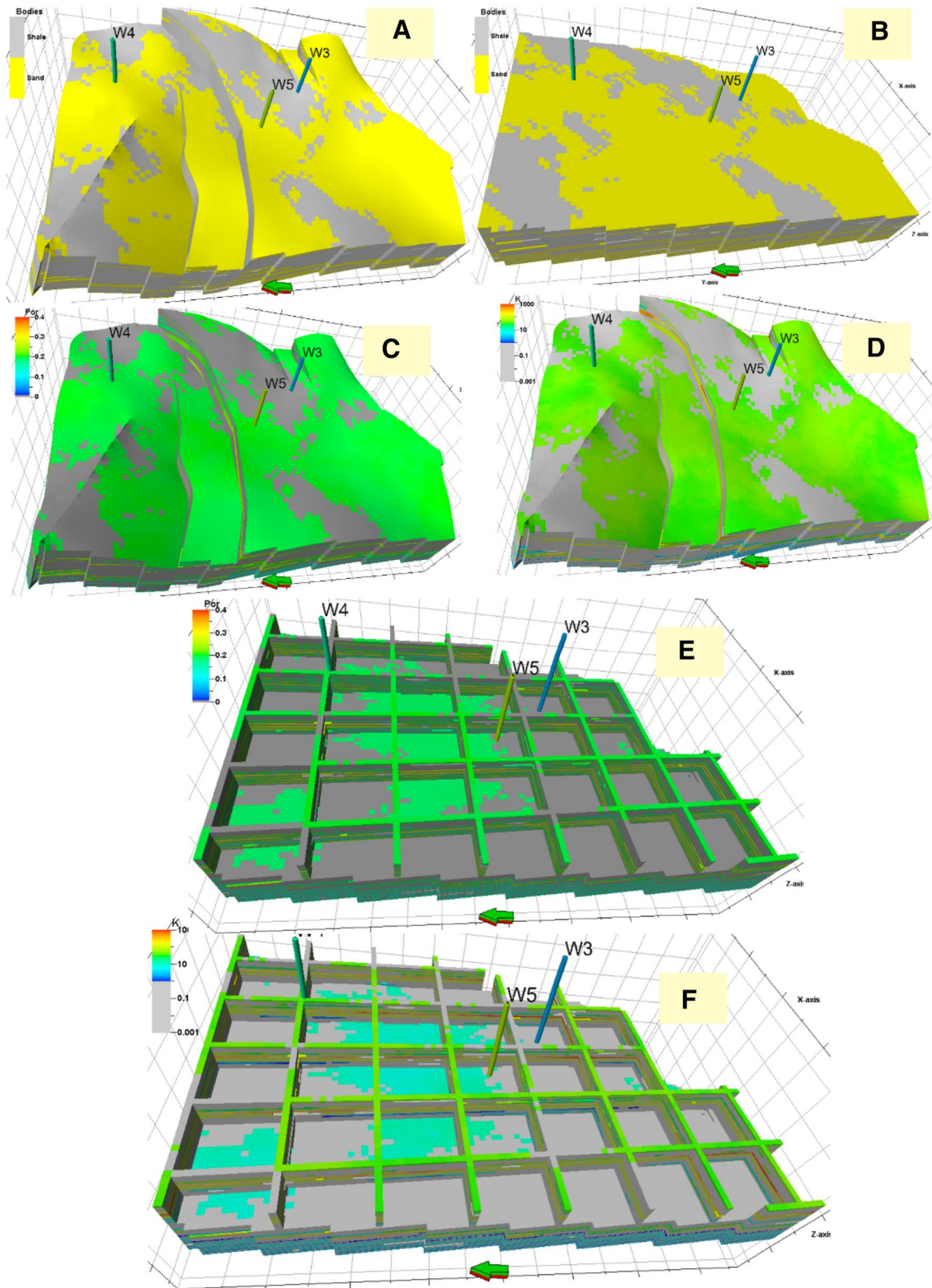
Fig. 8 3D property models and their sections established with the application of sequential indication simulation and sequential Gaussian simulation. **a** 3D depositional sand body model of the study area; **b** 3D depositional sand body model through toggle simbox view without taking fault into consideration; **c** 3D porosity model of the study area; **d** 3D permeability model of the study area; **e** three-dimensional fence model of **c** at *X*-axis (1, 1, 10), *Y*-axis (1, 1, 10), and *Z*-axis (15, 27, 27); **f** three-dimensional fence model of **d** at *X*-axis (1, 1, 10), *Y*-axis (1, 1, 10), and *Z*-axis (15, 27, 27)

Conclusions

The geology bodies and fault development of the study area are complex and multiplex, and thus this study aims to create a three-dimensional geological model which can realize 3D representations of complex reservoir data and geological modeling in the case of insufficient data. The 3D fault model and structural model are both established according to the unique structure map provided by CPEDC, reflecting the spatial geological characteristics of the study area and providing some guidance and help for oilfield development strategy to a certain extent. Fault-point data are essential to ensure the accuracy of fault modeling; the fault model established in this study is a general model and is suitable for the study area. In practical applications, the top structure map of layer is required to be available if possible, therefore, the fault evolution and changes in different formations can be obtained in detail, which will be helpful for fault modeling. Our application case is used in structure modeling with borehole sample data. Further work should be done by taking multiple factors into consideration, such as more complex geological objects, comprehensive modeling, manipulation methods, and visualization.

References

Bourdeau C, Lenti L, Martino S, Oguz O, Coccia S (2017) Comprehensive analysis of the local seismic response in the complex Büyükçekmece landslide area (Turkey) by engineering-geological and numerical modeling. Eng Geol 218:90–106

Calcagno P, Chilès JP, Courrioux G, Guillen A (2008) Geological modelling from field data and geological knowledge Part I. Modelling method coupling 3D potential-field interpolation and geological rules. Phys Earth Planet Inter 171:147–157

Chen FX (2008) The application of variogram in predicating braided river sandstone reservoir scale. J Chongqing Sci Technol 10:9–11 **(in Chinese)**

Chen XY, Doihara H, Nasu M (1995) A workstation for three-dimensional spatial data research. In: Proceeding, 4th international symposium of LIESMARS: towards three-dimensional, temporal and dynamic spatial data modeling and analysis, Wuhan, China, pp 42–51

Freulon XC, Dunderdale ID (1994) Integrating field measurements with conceptual models to produce a detailed 3D geological model. Soc Petrol Eng 28877:99–108

González-Garcia J, Jessell M (2016) A 3D geological model for the Ruiz-Tolima Volcanic Massif (Colombia): assessment of geological uncertainty using a stochastic approach based on Bézier curve design. Tectonophysics 687:139–157

Guo K, Shi J (2008) Variogram law study of Donghe sandstone reservoir in Tazhong 4 block. XINJIANG OIL GAS 4:4–8 (**in Chinese**)

Hélène B, Didier R (2016) Truncated Gaussian and derived methods. Math Geol 348:510–519

Houlding SW (1994) 3D geoscience modeling—computer techniques for geological characterization. Springer, New York, p 303

Lemon MA, Jones LN (2003) Building solid models from boreholes and user-defined cross sections. Comput Geosci 29:547–555

Martinez JL, Raiber M, Cendón DI (2017) Using 3D geological modelling and geochemical mixing models to characterise alluvial aquifer recharge sources in the upper Condamine River catchment, Queensland, Australia. Sci Total Environ 574:1–18

Mery N, Emery X, Cáceres A, Ribeiro D, Cunha E (2017) Geostatistical modeling of the geological uncertainty in an iron ore deposit. Ore Geol Rev 88:336–351

Pilout M, Tempfli K, Molenaar M (1994) A tetrahedron-based on 3D vector data model for geoinformation. In: Molenaar M, de Hoop S (eds) Advanced geographic data modeling, vol 40. Netherlands Geodetic Commission, Publications on Geodesy, Delft, pp 129–140

Shao YL (2012) 3D geological modeling under extremely complex geological conditions. J Comput 7(3):699–705

Shao YL, Zheng AL, He YB, Xiao KY (2011) 3D geological modeling and its application under complex geological conditions. Procedia Eng 12:41–46

Soubeyrand S (2017) Review of hierarchical modeling and analysis for spatial data by Banerjee, S., Carlin, B. P., and Gelfand, A. E. Math Geosci 49:677–678

Turner AK, Gable CW (2003) A review of geological modeling. Colorado School of Mines, Golden

Wang HT, Li YB, Xi JH (2010) Three-dimensional geological modeling technology and the application in city construction. Sci Surv Map 35(5):220–222 **(in Chinese)**

Yu XH (2002) Oil/gas reservoir sedimentology of clasolite series. Petroleum Industry Express, Beijing **(in Chinese)**

Zhang F, Li ZP, Wang HL, Wu J, Tan ZH (2007) Sands modeling constrained by high-resolution seismic data. J Zhejiang Univ Sci A 8(11):1858–1863

Publisher's Note Springer Nature remains neutral with regard to jurisdictional claims in published maps and institutional affiliations.

مدينة الملك عبدالعزيز
KACST للعلوم والتقنية

🙋 Springer